



# Electrochemical Determination of Nicotine in Tobacco Products Based on Biosynthesized Gold Nanoparticles

Yanqiu Jing<sup>1†</sup>, Shanghui Ning<sup>2†</sup>, Yu Guan<sup>3†</sup>, Mingfeng Cao<sup>2</sup>, Junju Li<sup>3</sup>, Li Zhu<sup>2</sup>, Qili Zhang<sup>3</sup>, Chuance Cheng<sup>1\*</sup> and Yong Deng<sup>2\*</sup>

<sup>1</sup> College of Tobacco Science, Henan Agricultural University, Zhengzhou, China, <sup>2</sup> Changde Branch of Hunan Tobacco Corporation, Changde, China, <sup>3</sup> Sichuan of China National Tobacco Corporation, Chengdu, China

## OPEN ACCESS

### Edited by:

Hassan Karimi-Maleh,  
University of Electronic Science and  
Technology of China, China

### Reviewed by:

Yuhong Zheng,  
Jiangsu Province and Chinese  
Academy of Sciences, China  
Sadegh Salmanpour,  
Islamic Azad University Sari  
Branch, Iran

### \*Correspondence:

Yanqiu Jing  
jingyanqiu72t@henau.edu.cn  
Chuance Cheng  
chuancecheng\_hau@163.com  
Yong Deng  
mu94237937@163.com

<sup>†</sup>These authors have contributed  
equally to this work

### Specialty section:

This article was submitted to  
Electrochemistry,  
a section of the journal  
Frontiers in Chemistry

**Received:** 09 August 2020

**Accepted:** 04 September 2020

**Published:** 20 October 2020

### Citation:

Jing Y, Ning S, Guan Y, Cao M, Li J,  
Zhu L, Zhang Q, Cheng C and Deng Y  
(2020) Electrochemical Determination  
of Nicotine in Tobacco Products  
Based on Biosynthesized Gold  
Nanoparticles.  
Front. Chem. 8:593070.  
doi: 10.3389/fchem.2020.593070

In this work, gold nanoparticles were biosynthesized via *Plectranthus amboinicus* leaf extract as the reducing agent. A series of techniques were used for sample analysis. The biosynthesized gold nanoparticles (bAuNPs) are a uniform size with a spherical shape. The FTIR analysis reveals the presence of many oxygen-containing functional groups on the bAuNP surface. The cyclic voltammetry and electrochemical impedance spectroscopic characterizations reveal that while the bAuNPs have a slightly lower conductivity than chemically synthesized AuNPs (cAuNPs). However, the bAuNPs have a superior electrocatalytic performance toward nicotine reduction. After optimization, the bAuNP-modified SPE could detect nicotine linearly from 10 to 2,000  $\mu$ M with a low detection limit of 2.33  $\mu$ M. In addition, the bAuNPs/SPE have been successfully used for nicotine-containing-product analysis.

**Keywords:** biosynthesis, nicotine, gold nanoparticle, electrochemical sensor, *Plectranthus amboinicus*

## INTRODUCTION

Nicotine is an alkaloid found in the Solanaceae family and is an important ingredient in tobacco. Currently, the fact that smoking is harmful to health has become common sense. The main active ingredient of cigarettes is nicotine. When nicotine enters the alveoli, it is quickly absorbed and causes serious respiratory diseases and cancer. The data show that the number of deaths caused by smoking each year is up to several million. Therefore, analysis of the quantity of nicotine that is present in tobacco products is very important to the tobacco and pharmaceutical industries. In recent years, methods for the analysis of nicotine have been continuously developed. In addition to traditional chemical methods and titration methods, electrochemical methods, atomic absorption spectrometry, gas chromatography, spectrophotometry, and high-performance liquid chromatography have all been used for the analytical determination of nicotine. Among these techniques, electrochemical-based methods have been found to be more portable with a quick detection procedure and low cost (Fu et al., 2019a; Feng et al., 2020; Hojjati-Najafabadi et al., 2020; Hou et al., 2020; Karimi-Maleh et al., 2020a,b; Naderi Asrami et al., 2020; Xu et al., 2020). However, the common commercial electrode is not sensitive enough for determination of nicotine at low concentrations. Therefore, electrode surface modification has been used for improving the sensitivity of electrochemical methods. For example, Shehata and coworkers demonstrated the use of a nano-TiO<sub>2</sub>-modified carbon paste

sensor for nicotine detection (Shehata et al., 2016). Wang and coworkers demonstrated a sensitive nicotine electrochemical sensor based on multiwalled carbon nanotube–alumina-coated silica (Wang et al., 2009). Yu and coworkers reported an electrochemical nicotine sensor based on a multiwalled carbon nanotube/graphene composite (Yu et al., 2016).

Although these prior works demonstrated excellent performance toward electrochemical detection, the chemical synthesis of the electrode modifiers utilized strong reducing agents or toxic reagents (Fu et al., 2019b). Currently, the green synthesis of metal nanoparticles is an interesting issue in the field of nanoscience. There is also growing attention to the biosynthesis of metal nanoparticles using organisms (Hulkoti and Taranath, 2014; Ahmed et al., 2017; Fu et al., 2020a). Noble metal nanoparticles have been synthesized using various plant extracts. For example, Zheng et al. reported a facile biosynthetic approach for Ag NP preparation using *Plectranthus amboinicus* leaf extract (Zheng et al., 2017). Medda and coworkers reported a biosynthesis of Ag NPs using *Aloe vera* leaf extract (Medda et al., 2015). Most of the biosynthesized noble metal nanoparticles were applied for antibacterial and catalytic applications (El-Seedi et al., 2019; Otari et al., 2019; Spagnoletti et al., 2019; Fu et al., 2020b;

Ramteke et al., 2020). In this work, we attempted to extend the application to biosynthesized Au NPs for electrochemical sensing. Gold nanoparticles have attracted increasing attention due to their unique properties in multidisciplinary research fields (Zhang and Hu, 2019; Li et al., 2020). Its nanostructures have been used for fabrication of optical devices (Noguez and Garzón, 2009), catalysis (Corma and Garcia, 2008), surface-enhanced Raman scattering (SERS) (Wang et al., 2016), biological labeling (Dalal et al., 2016), bioimaging (Sun et al., 2018), and drug delivery and antimicrobial agents (Manzano and Vallet-Regi, 2020). Recently, syntheses of Au and Ag nanoparticles using extracts of cinnamomum camphora leaf (Huang et al., 2007), phyllanthin (Kasthuri et al., 2009), or edible mushroom (Philip, 2009) as reducing and capping agents have been reported. In this article, we further investigate the electrochemical properties of the *Plectranthus amboinicus* leaf extract-synthesized Ag NPs toward nicotine.

## EXPERIMENTS

*Plectranthus amboinicus* plants were purchased from a local nursery of Zhengzhou, China.  $\text{HAuCl}_4$  and nicotine

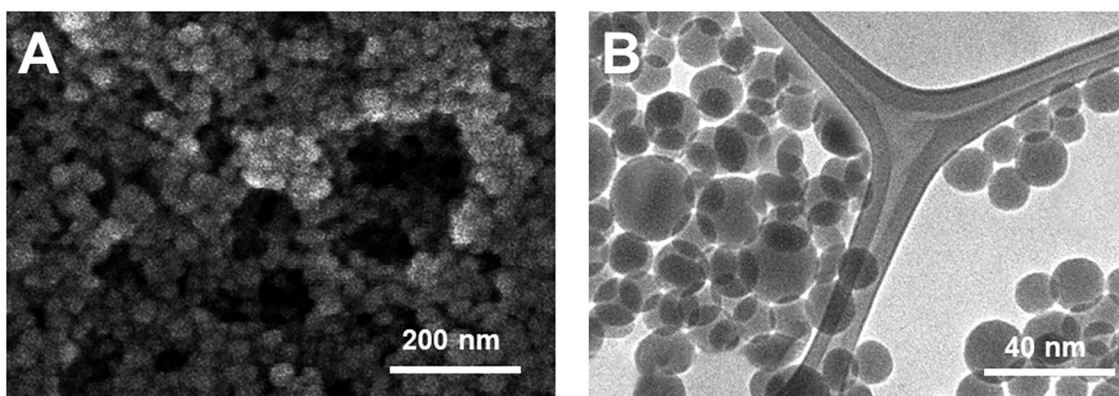


FIGURE 1 | (A) SEM and (B) TEM image of bAuNPs.

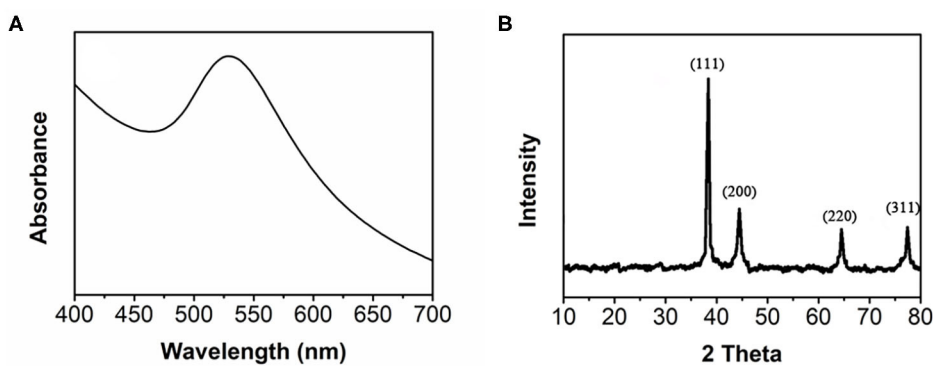


FIGURE 2 | (A) UV-vis spectrum and (B) XRD pattern of bAuNPs.

were purchased from Sigma-Aldrich. All other chemicals were analytical grade reagents and were used without further purification.

Ten milliliter of *Plectranthus amboinicus* leaf extract was added into a 0.1 M  $\text{HAuCl}_4$  solution and stirred continuously at 70°C for 5 h. The gray precipitate was collected using centrifugation. Chemically synthesized Au NPs were prepared using the same quantity of gold precursor and 1 mL of sodium borohydride (0.5 mM) as the reducing agent.

For the electrochemical study, a GCE (3 mm in diameter) was polished with an alumina-water slurry and then rinsed with water. Then, 5  $\mu\text{L}$  of dispersion catalyst (0.5 mg/mL) was dropped onto the GCE surface and dried naturally. Electrochemical measurements were performed on a CHI660A electrochemical Workstation using a three-electrode system. A platinum wire was used as the

auxiliary electrode and Ag/AgCl (3M KCl) was used as the reference electrode.

## RESULTS AND DISCUSSION

The morphology of the biosynthesized AuNPs (bAuNPs) was characterized using SEM and TEM. **Figure 1A** shows the SEM image of the bAuNPs. It can be observed that the bAuNPs were spherical in shape with a diameter of <20 nm (**Figure 1A**). The boundary between the particles can be clearly observed, suggesting the possibility that biomolecule functional groups are on the bAuNP surfaces, preventing aggregation. TEM characterization provides more detailed morphology information. As shown in **Figure 1B**, the average diameter of the bAuNPs is 14 nm, based on the calculation of 50 individual particles. With the exception of some larger particles, most bAuNPs are a uniform size.

The formation of bAuNPs was then confirmed using UV-Vis spectroscopy and XRD. As shown in **Figure 2A**, the UV-Vis spectrum of the bAuNPs shows a peak located at  $\sim 525$  nm, indicating excitations from the surface plasmon vibration of the AuNPs (Vilas et al., 2016). The sharp shape of the UV-Vis peak also suggests the uniform size of the bAuNPs. **Figure 2B** shows the XRD pattern of the bAuNPs. As shown in the figure, the pattern exhibits several peaks located at the scan angles  $38.29^\circ$ ,  $44.42^\circ$ ,  $64.74^\circ$ , and  $77.67^\circ$ , corresponding to the (111), (200), (220), and (311) planes, respectively, of standard gold metal ( $\text{Au}^0$ ) (Yang et al., 2014). No extra peaks were found in the XRD pattern, suggesting no impurity crystals were formed during the biosynthesis process.

The presence of the surface functional groups on the bAuNPs was confirmed using FTIR spectroscopy. **Figure 3** shows the FTIR spectrum of the bAuNPs with the *Plectranthus amboinicus* leaf extract. The spectrum of the leaf extract displays a series of absorbance bands ranging from 700 to 2,000  $\text{cm}^{-1}$ . The absorbance bands at 1,334 and 1,220  $\text{cm}^{-1}$  can be ascribed to the C-O stretching frequencies corresponding to polysaccharides and polyols. The polysaccharides and polyols commonly exhibit

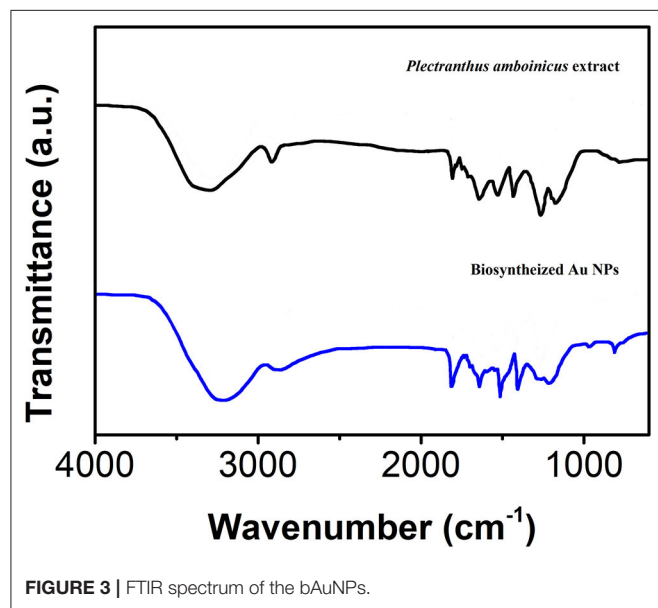


FIGURE 3 | FTIR spectrum of the bAuNPs.

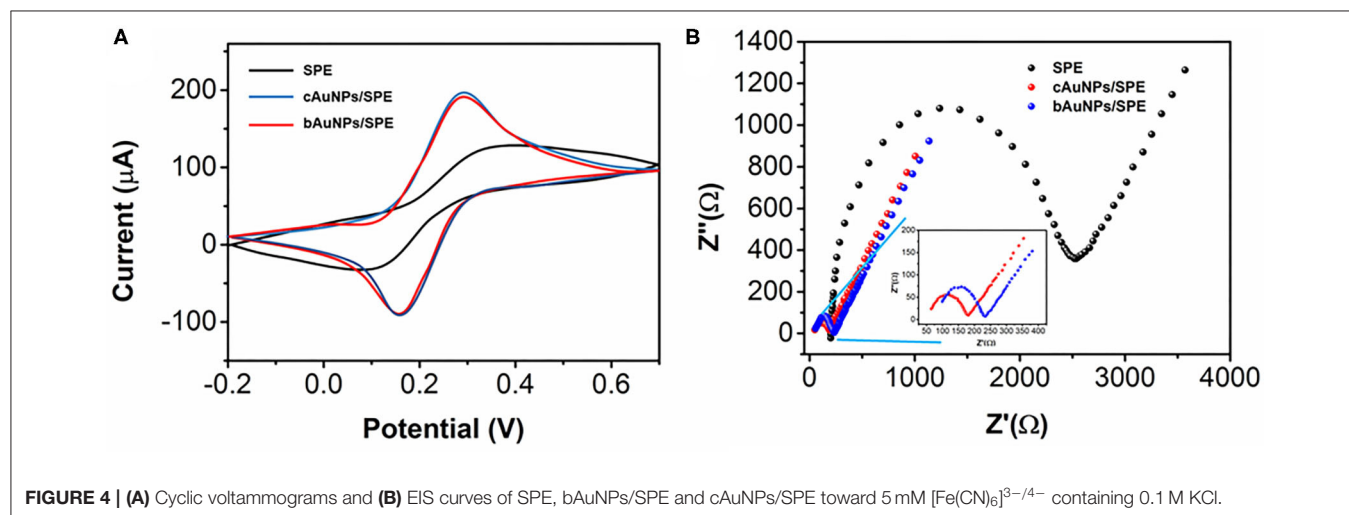


FIGURE 4 | (A) Cyclic voltammograms and (B) EIS curves of SPE, bAuNPs/SPE and cAuNPs/SPE toward 5 mM  $[\text{Fe}(\text{CN})_6]^{3-/4-}$  containing 0.1 M KCl.

weak reducibility, which can be used for Au precursor reduction (Begum et al., 2009). In addition, an absorbance band located at  $879\text{ cm}^{-1}$  corresponds to the C-N vibrations of the nitroso groups, which are typically present when nanomaterial surfaces are capped by biomolecules (Slocik and Naik, 2017; Wang et al., 2018; Shamsadin-Azad et al., 2019; Karimi-Maleh et al., 2020; Karthikeyan et al., 2020).

The electrochemical properties of the bAuNPs were compared with chemically synthesized AuNPs (cAuNPs) by cyclic voltammetry using a  $[\text{Fe}(\text{CN})_6]^{3-/4-}$  probe. As shown in **Figure 4A**, the bare SPE has well-defined redox peaks at 0.32 and 0.11 V, while both the cAuNPs/SPE and the bAuNPs/SPE exhibit smaller peak-peak separation. Specifically, the cAuNPs/SPE has redox peaks at 0.26 and 0.18 V, while the bAuNPs/SPE has redox peaks at 0.25 and 0.18 V. The results indicate that modification by either of the synthesized AuNPs significantly enhances the electroconductivity of the SPE. It can be observed

that the bAuNPs/SPE has a slight lower oxidation peak response compared with that of the cAuNPs/SPE, suggesting that AuNPs biosynthesized using *Plectranthus amboinicus* leaf extract as the reducing agent could be of a competitive quality when compared to common chemically synthesized AuNPs. Electrochemical impedance spectroscopy (EIS) was used for further analysis. As shown in **Figure 4B**, the bare SPE shows a larger capacitive loop than both of the AuNP modified SPEs. As shown in the inset of the **Figure 4B**, the cAuNPs/SPE exhibits a slightly smaller capacitive loop than that of the bAuNPs/SPE, suggesting that the cAuNPs/SPE has a superior electroconductivity. This observation is in good agreement with the results deduced from CV characterization.

Although the electroconductivity of the bAuNPs/SPE is not as good as the cAuNPs/SPE, the bAuNPs/SPE has a superior electrocatalytic response toward nicotine. As shown in **Figure 5**, bare SPE shows negligible reduction toward 0.5 mM nicotine. In contrast, both bAuNPs/SPE and cAuNPs/SPE exhibit a well-defined reduction peak toward 0.5 mM nicotine, suggesting that the AuNPs could effectively trigger the electrocatalytic reduction of nicotine. More specifically, the cAuNPs/SPE exhibits a reduction peak at  $-0.86\text{ V}$  with a current response of  $60.77\text{ }\mu\text{A}$ , while the bAuNPs/SPE exhibits a reduction peak at  $-0.80\text{ V}$  with a current response of  $87.62\text{ }\mu\text{A}$ . The lower reduction potential with a higher current response indicates the bAuNPs/SPE exhibits a superior electrocatalytic response toward nicotine compared with that of the cAuNPs/SPE. The superior electrocatalytic performance could be ascribed to the presence of the biomolecules of the bAuNPs/SPE surface. As indicated in the FTIR characterization, these molecules offer many oxygen-containing functional groups to the bAuNPs, which could be used for binding nicotine and result in a higher current response. Moreover, as reported in the literature (Huang et al., 2018; Liang et al., 2018; Zhu et al., 2019), oxygen-containing groups could trigger the electrocatalytic reaction during the scan. We also conducted cyclic voltammetry of the bAuNPs/SPE in the absence of nicotine. No noticeable peak can be found in the CV profile, suggesting that the peak located at  $-0.80\text{ V}$  does indeed belong to the nicotine reduction.

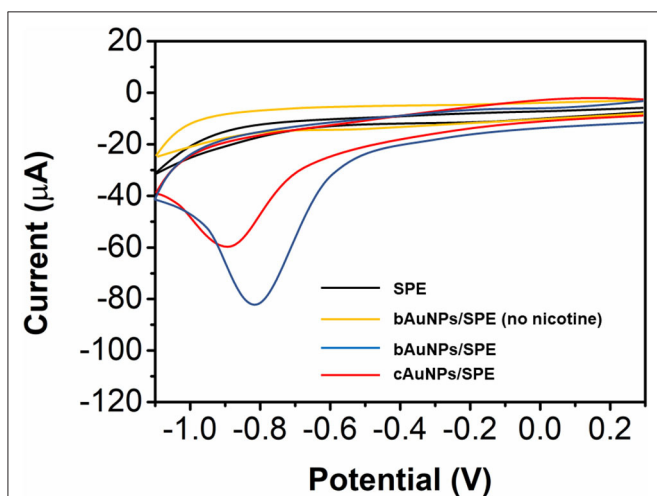


**FIGURE 5** | Cyclic voltammograms of the bare SPE, cAuNPs/SPE and bAuNPs/SPE toward 0.5 mM nicotine.

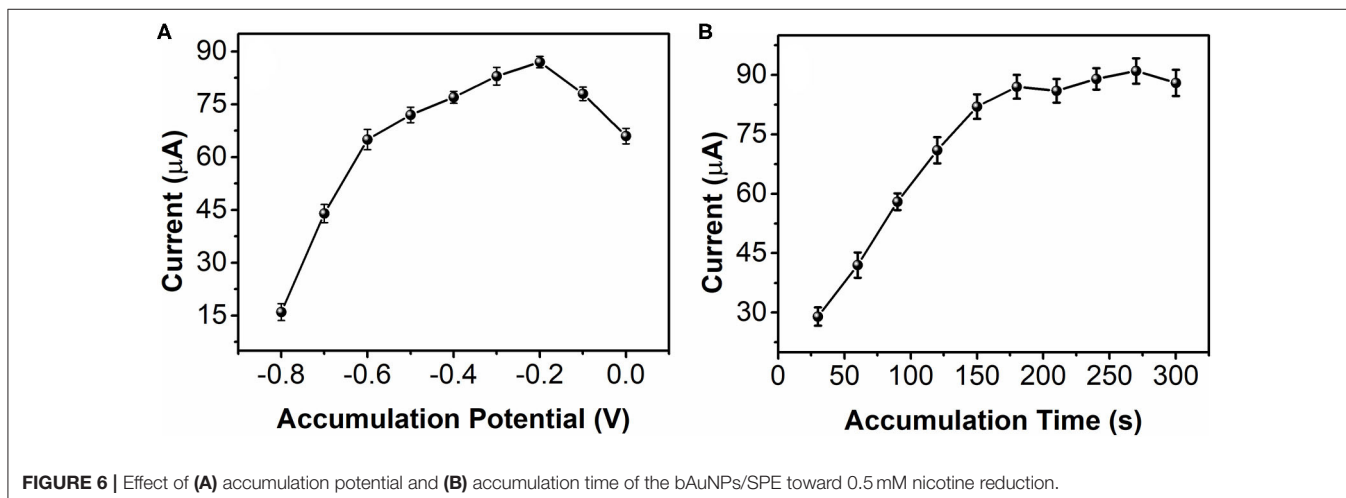


**FIGURE 6** | Effect of (A) accumulation potential and (B) accumulation time of the bAuNPs/SPE toward 0.5 mM nicotine reduction.

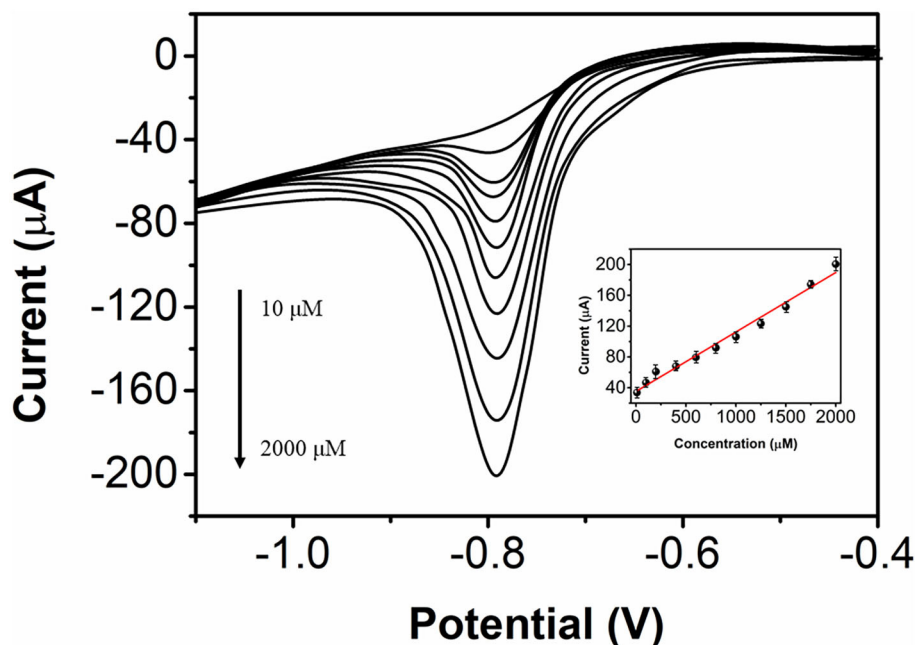


**FIGURE 7** | Differential pulse voltammograms of the bAuNPs/SPE toward nicotine from 10  $\mu\text{M}$  to 2 mM.

**TABLE 1** | Electrochemical nicotine sensor performance comparison.

Electrode	Linear detection range	Detection limit	References
Nitrogen-doped graphene/GCE	0–200 $\mu\text{M}$	0.27 $\mu\text{M}$	Li et al., 2017
PoPD/GCE	0.000183–1.01 $\mu\text{M}$	55.00 pM	Liang et al., 2012
Boron-doped diamond electrode	0.5–200 $\mu\text{M}$	0.30 $\mu\text{M}$	Švorc et al., 2014
RGO/DPA/PGE	131–1,900 $\mu\text{M}$	7.60 $\mu\text{M}$	Jing et al., 2017
bAuNPs/SPE	10–2,000 $\mu\text{M}$	2.33 $\mu\text{M}$	This work

Accumulation is an important process for enhancing electrochemical sensing. **Figure 6A** shows the effect of 0.5 mM nicotine reduction at bAuNPs/SPE with different accumulation potentials. The results suggest that accumulation at a more negative potential does not improve the sensing performance. The reduction increases along with the accumulation potential decreases from  $-0.8$  to  $-0.2$  V. The maximum current can be noticed at  $-0.2$  V. In addition, further decreasing the accumulation potential can reverse the sensing performance. Therefore,  $-0.2$  V was selected for nicotine reduction. Accumulation time is another important factor. As shown in **Figure 6B**, the current response of the nicotine reduction increases as the accumulation time increases. A significant current increase can be observed as the accumulation time increases from 30 to 150 s. The enhancement speed of the current response was decreased after 150 s, and especially after

180 s accumulation time. Therefore, 180 s was used for the accumulation time.

The determination performance of bAuNPs/SPE toward nicotine was also studied using differential pulse voltammetry (DPV). **Figure 7** shows the DPV profiles of the bAuNPs/SPE toward nicotine at nicotine concentrations of 10  $\mu\text{M}$  to 2 mM, while the inset shows the plot of current response against nicotine concentration. A linear regression was found, and the equation can be expressed as  $I(\mu\text{A}) = 0.07722(\text{concentration}) + 35.25039$  ( $R = 0.99$ ). The limit of detection was calculated to be 2.33  $\mu\text{M}$  based on a signal-to-noise ratio of 3. **Table 1** shows the comparison of the performance of the proposed electrochemical nicotine sensor with performances in previous reports. As shown in the table, the bAuNPs/SPE exhibits a wider electrochemical sensing performance compared with other reported performances, which is favorable for nicotine analysis in tobacco products.

The anti-interference property of the bAuNPs/SPE was also studied. **Figure 8** shows the successive addition of 0.5 mM nicotine, glucose, uric acid, ascorbic acid, dopamine, norepinephrine, and tyrosine. It can be seen that all interference molecules showed negligible effects on the nicotine sensing (current changes of  $<5\%$ ). The results suggest that the proposed bAuNPs/SPE has a good anti-interference property to nicotine sensing.

The reproducibility of the bAuNPs/SPE was tested with seven individually prepared electrodes. **Figure 9A** shows the current responses of the seven electrodes toward 0.5 mM nicotine. The RSD is calculated to be 4.41%, suggesting that the proposed bAuNPs/SPE has a stable

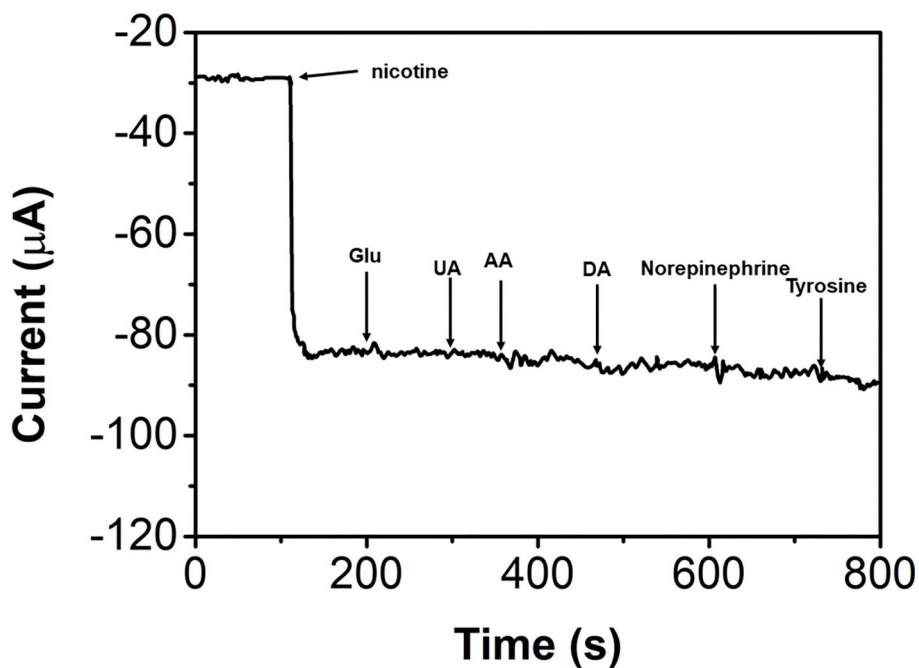


**FIGURE 8** | I-T response of the bAuNPs/SPE with successive addition of 0.5 mM nicotine, glucose, uric acid, ascorbic acid, dopamine, norepinephrine and tyrosine.

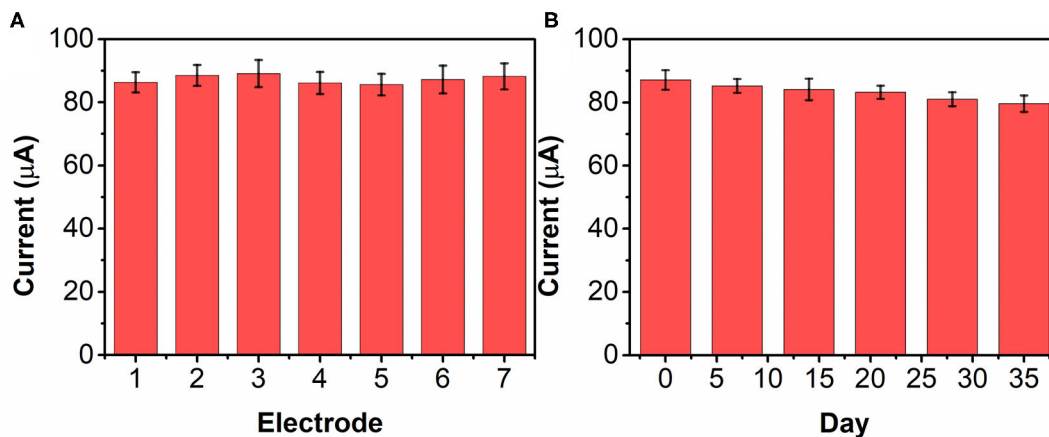


**FIGURE 9** | (A) Reproducibility of seven individual bAuNPs/SPE toward 0.2 mM nicotine detection. (B) Long-term stability test of bAuNPs/SPE.

performance. The long-term stability of the bAuNPs/SPE was also tested. As shown in **Figure 9B**, the bAuNPs/SPE retain more than 85% of original performance after 35 days of storage at room temperature, suggesting acceptable long-term stability.

Two brands of cigarette and an E-cigarette liquid refill were used as real test samples. Nicotine was extracted from the cigarette samples using ethanol. The detection results are summarized in **Table 2**. A standard addition method was adopted for determining the recovery rate for the proposed electrochemical-sensing strategy. As shown in **Table 2**, the bAuNPs/SPE show a well-resolved

performance and recovery rate, suggesting the potential of the bAuNPs/SPE to be used for commercial nicotine containing product analysis.

## CONCLUSIONS

In conclusion, bAuNPs have been successfully biosynthesized using *Plectranthus amboinicus* leaf extract as the reducing agent. The formed bAuNPs have a uniform size with a spherical shape. Characterizations indicate the proposed biosynthesis method could be used to prepare AuNPs with a high purity. The FTIR spectrum confirms the functional

**TABLE 2** | Electrochemical determination of nicotine concentrations in two brands of cigarette and an E-cigarette liquid refill using bAuNPs/SPE.

Sample	Addition ( $\mu\text{M}$ )	Found ( $\mu\text{M}$ )	RSD (%)	Recovery (%)
Cigarette 1	0	22.4	3.4	–
	50	73.2	5.5	101.1
	100	123.2	2.6	100.7
Cigarette 2	0	14.4	3.3	–
	50	66.3	3.6	103.0
	100	111.4	7.1	97.4
E-cigarette	0	29.7	4.3	–
	50	77.4	2.9	97.1
	100	132.2	4.2	101.9

groups that are present on the bAuNPs surface. Although the conductivity of the bAuNPs is slightly lower than that of the cAuNPs, the electrocatalytic performance of the bAuNPs is superior. The bAuNP-modified SPE performed an effective

electrocatalytic reduction of nicotine. Under optimum conditions, the bAuNPs/SPE could detect nicotine over a linear range from 10 to 2,000  $\mu\text{M}$  with a low detection limit of 2.33  $\mu\text{M}$ . In addition, the bAuNPs/SPE have been successfully used for nicotine-containing-product analysis.

## DATA AVAILABILITY STATEMENT

The original contributions presented in the study are included in the article/supplementary material, further inquiries can be directed to the corresponding authors.

## AUTHOR CONTRIBUTIONS

YJ, SN, and YG conceived of the study. YJ, CC, and YD supervised the development program and collected materials characterization. QZ, MC, and JL received and curated samples and analytical records. SN, LZ, and YJ wrote the manuscript. All authors read and approved of the manuscript.

## REFERENCES

- Ahmed, S., Chaudhry, S. A., and Ikram, S. (2017). A review on biogenic synthesis of ZnO nanoparticles using plant extracts and microbes: a prospect towards green chemistry. *J. Photochem. Photobiol. B* 166, 272–284. doi: 10.1016/j.jphotobiol.2016.12.011
- Begum, N. A., Mondal, S., Basu, S., Laskar, R. A., and Mandal, D. (2009). Biogenic synthesis of Au and Ag nanoparticles using aqueous solutions of Black Tea leaf extracts. *Colloids Surf. B Biointerfaces* 71, 113–118. doi: 10.1016/j.colsurfb.2009.01.012
- Corma, A., and Garcia, H. (2008). Supported gold nanoparticles as catalysts for organic reactions. *Chem. Soc. Rev.* 37, 2096–2126. doi: 10.1039/b707314n
- Dalal, C., Saha, A., and Jana, N. R. (2016). Nanoparticle multivalency directed shifting of cellular uptake mechanism. *J. Phys. Chem. C* 120, 6778–6786. doi: 10.1021/acs.jpcc.5b11059
- El-Seedi, H. R., El-Shabasy, R. M., Khalifa, S. A., Saeed, A., Shah, A., Shah, R., et al. (2019). Metal nanoparticles fabricated by green chemistry using natural extracts: biosynthesis, mechanisms, and applications. *RSC Adv.* 9, 24539–24559. doi: 10.1039/C9RA02225B
- Feng, Y., Wei, Z., and Zhang, J. (2020). Determination of ursolic acid in extracts from *ligustri lucidum* fruit using an electrochemical method. *Front. Chem.* 8:444. doi: 10.3389/fchem.2020.00444
- Fu, L., Wang, A., Xie, K., Zhu, J., Chen, F., Wang, H., et al. (2020a). Electrochemical detection of silver ions by using sulfur quantum dots modified gold electrode. *Sens. Actuators B Chem.* 304:127390. doi: 10.1016/j.snb.2019.127390
- Fu, L., Wu, M., Zheng, Y., Zhang, P., Ye, C., Zhang, H., et al. (2019a). Lycoris species identification and infrageneric relationship investigation via graphene enhanced electrochemical fingerprinting of pollen. *Sens. Actuators B Chem.* 298:126836. doi: 10.1016/j.snb.2019.126836
- Fu, L., Xie, K., Wang, A., Lyu, F., Ge, J., Zhang, L., et al. (2019b). High selective detection of mercury (II) ions by thioether side groups on metal-organic frameworks. *Anal. Chim. Acta* 1081, 51–58. doi: 10.1016/j.aca.2019.06.055
- Fu, L., Zheng, Y., Zhang, P., Zhang, H., Xu, Y., Zhou, J., et al. (2020b). Development of an electrochemical biosensor for phylogenetic analysis of *Amaryllidaceae* based on the enhanced electrochemical fingerprint recorded from plant tissue. *Biosens. Bioelectron.* 159:112212. doi: 10.1016/j.bios.2020.112212
- Hojjati-Najafabadi, A., Rahmanpour, M. S., Karimi, F., Zabihi-Feyzaba, H., Malekmohammad, S., Agarwal, S., et al. (2020). Determination of tert-butylhydroquinone using a nanostructured sensor based on CdO/SWCNTs and ionic liquid. *Int. J. Electrochem. Sci.* 15, 6969–6980. doi: 10.20964/2020.07.85
- Hou, K., Zhao, P., Chen, Y., Li, G., Lin, Y., Chen, D., et al. (2020). Rapid detection of *bifidobacterium bifidum* in feces sample by highly sensitive quartz crystal microbalance immunosensor. *Front. Chem.* 8:548. doi: 10.3389/fchem.2020.00548
- Huang, D., Li, S., Zhang, X., Luo, Y., Xiao, J., and Chen, H. (2018). A novel method to significantly boost the electrocatalytic activity of carbon cloth for oxygen evolution reaction. *Carbon* 129, 468–475. doi: 10.1016/j.carbon.2017.12.046
- Huang, J., Li, Q., Sun, D., Lu, Y., Su, Y., Yang, X., et al. (2007). Biosynthesis of silver and gold nanoparticles by novel sundried *Cinnamomum camphoraleaf*. *Nanotechnology* 18:105104. doi: 10.1088/0957-4484/18/10/105104
- Hulkoti, N. I., and Taranath, T. C. (2014). Biosynthesis of nanoparticles using microbes—A review. *Colloids Surf. B Biointerfaces* 121, 474–483. doi: 10.1016/j.colsurfb.2014.05.027
- Jing, Y., Yu, B., Li, P., Xiong, B., Cheng, Y., Li, Y., et al. (2017). Synthesis of graphene/DPA composite for determination of nicotine in tobacco products. *Sci. Rep.* 7:14332. doi: 10.1038/s41598-017-13716-2
- Karimi-Maleh, H., Karimi, F., Alizadeh, M., and Sanati, A. L. (2020a). Electrochemical sensors, a bright future in the fabrication of portable kits in analytical systems. *Chem. Rec.* 20, 682–692. doi: 10.1002/tcr.201900092
- Karimi-Maleh, H., Karimi, F., Malekmohammadi, S., Zakariae, N., Esmaili, R., Rostamnia, S., et al. (2020b). An amplified voltammetric sensor based on platinum nanoparticle/polyoxometalate/two-dimensional hexagonal boron nitride nanosheets composite and ionic liquid for determination of N-hydroxysuccinimide in water samples. *J. Mol. Liq.* 310:113185. doi: 10.1016/j.molliq.2020.113185
- Karimi-Maleh, H., Karimi, F., Orooji, Y., Mansouri, G., Razmjou, A., Aygun, A., et al. (2020c). A new nickel-based co-crystal complex electrocatalyst amplified by NiO doped Pt nanostructure hybrid; a highly sensitive approach for determination of cysteamine in the presence of serotonin. *Sci. Rep.* 10:11699. doi: 10.1038/s41598-020-68663-2
- Karthikeyan, C., Varaprasad, K., Akbari-Fakhrabadi, A., Hameed, A. S. H., and Sadiku, R. (2020). Biomolecule chitosan, curcumin and ZnO-based antibacterial nanomaterial, via a one-pot process. *Carbohydr. Polym.* 249:116825. doi: 10.1016/j.carbpol.2020.116825
- Kasthuri, J., Kathiravan, K., and Rajendiran, N. (2009). Phyllanthin-assisted biosynthesis of silver and gold nanoparticles: a novel biological approach. *J. Nanoparticle Res.* 11, 1075–1085. doi: 10.1007/s11051-008-9494-9
- Li, C., Huang, R., and Shi, X. (2020). Biosynthesis of Cu nanoparticles supported on carbon nanotubes and its catalytic performance under different test conditions. *J. Chem. Technol. Biotechnol.* 95, 1511–1518. doi: 10.1002/jctb.6344
- Li, X., Zhao, H., Shi, L., Zhu, X., Lan, M., Zhang, Q., et al. (2017). Electrochemical sensing of nicotine using screen-printed carbon electrodes modified with nitrogen-doped graphene sheets. *J. Electroanal. Chem.* 784, 77–84. doi: 10.1016/j.jelechem.2016.12.009

- Liang, J., Han, F., and Chen, Y. (2012). An electrochemical method for high sensitive detection of nicotine and its interaction with bovine serum albumin. *Electrochem. Commun.* 24, 93–96. doi: 10.1016/j.elecom.2012.08.024
- Liang, J., Li, C., Li, W., Qi, J., and Liang, C. (2018). Microwave-assisted polyol preparation of reduced graphene oxide nanoribbons supported platinum as a highly active electrocatalyst for oxygen reduction reaction. *J. Appl. Electrochem.* 48, 1069–1080. doi: 10.1007/s10800-018-1235-x
- Manzano, M., and Vallet-Regí, M. (2020). Mesoporous silica nanoparticles for drug delivery. *Adv. Funct. Mater.* 30:1902634. doi: 10.1002/adfm.201902634
- Medda, S., Hajra, A., Dey, U., Bose, P., and Mondal, N. K. (2015). Biosynthesis of silver nanoparticles from Aloe vera leaf extract and antifungal activity against *Rhizopus* sp. and *Aspergillus* sp. *Appl. Nanosci.* 5, 875–880. doi: 10.1007/s13204-014-0387-1
- Naderi Asrami, P., Aberoomand Azar, P., Saber Tehrani, M., and Mozaffari, S. A. (2020). Glucose oxidase/nano-ZnO/thin film deposit FTO as an innovative clinical transducer: a sensitive glucose biosensor. *Front. Chem.* 8:503. doi: 10.3389/fchem.2020.00503
- Noguez, C., and Garzón, I. L. (2009). Optically active metal nanoparticles. *Chem. Soc. Rev.* 38, 757–771. doi: 10.1039/b800404h
- Otari, S. V., Patel, S. K., Kalia, V. C., Kim, I.-W., and Lee, J.-K. (2019). Antimicrobial activity of biosynthesized silver nanoparticles decorated silica nanoparticles. *Indian J. Microbiol.* 59, 379–382. doi: 10.1007/s12088-019-00812-2
- Philip, D. (2009). Biosynthesis of Au, Ag and Au–Ag nanoparticles using edible mushroom extract. *Spectrochim. Acta. A. Mol. Biomol. Spectrosc.* 73, 374–381. doi: 10.1016/j.saa.2009.02.037
- Ramteke, L., Gawali, P., Jadhav, B., and Chopade, B. (2020). Comparative study on antibacterial activity of metal ions, monometallic and alloy noble metal nanoparticles against nosocomial pathogens. *BioNanoScience.* 3, 1–19. doi: 10.1007/s12668-020-00771-9
- Shamsadin-Azad, Z., Taher, M. A., Cheraghi, S., and Karimi-Maleh, H. (2019). A nanostructure voltammetric platform amplified with ionic liquid for determination of tert-butylhydroxyanisole in the presence kojic acid. *J. Food Meas. Charact.* 13, 1781–1787. doi: 10.1007/s11694-019-00096-6
- Shehata, M., Azab, S., Fekry, A., and Ameer, M. (2016). Nano-TiO<sub>2</sub> modified carbon paste sensor for electrochemical nicotine detection using anionic surfactant. *Biosens. Bioelectron.* 79, 589–592. doi: 10.1016/j.bios.2015.12.090
- Slocik, J. M., and Naik, R. R. (2017). Sequenced defined biomolecules for nanomaterial synthesis, functionalization, and assembly. *Syst. Biol. Nanobiotech.* 46, 7–13. doi: 10.1016/j.copbio.2016.11.025
- Spagnoletti, F. N., Spedalieri, C., Kronberg, F., and Giacometti, R. (2019). Extracellular biosynthesis of bactericidal Ag/AgCl nanoparticles for crop protection using the fungus *Macrophomina phaseolina*. *J. Environ. Manage.* 231, 457–466. doi: 10.1016/j.jenvman.2018.10.081
- Sun, S.-K., Wang, H.-F., and Yan, X.-P. (2018). Engineering persistent luminescence nanoparticles for biological applications: from biosensing/bioimaging to theranostics. *Acc. Chem. Res.* 51, 1131–1143. doi: 10.1021/acs.accounts.7b00619
- Švorc, L., Stanković, D. M., and Kalcher, K. (2014). Boron-doped diamond electrochemical sensor for sensitive determination of nicotine in tobacco products and anti-smoking pharmaceuticals. *Diam. Relat. Mater.* 42, 1–7. doi: 10.1016/j.diamond.2013.11.012
- Vilas, V., Philip, D., and Mathew, J. (2016). Biosynthesis of Au and Au/Ag alloy nanoparticles using *Coleus aromaticus* essential oil and evaluation of their catalytic, antibacterial and antiradical activities. *J. Mol. Liq.* 221, 179–189. doi: 10.1016/j.molliq.2016.05.066
- Wang, S.-J., Liaw, H.-W., and Tsai, Y.-C. (2009). Low potential detection of nicotine at multiwalled carbon nanotube–alumina-coated silica nanocomposite. *Electrochem. Commun.* 11, 733–735. doi: 10.1016/j.elecom.2009.01.026
- Wang, Y., Kang, S., Khan, A., Ruttner, G., Leigh, S. Y., Murray, M., et al. (2016). Quantitative molecular phenotyping with topically applied SERS nanoparticles for intraoperative guidance of breast cancer lumpectomy. *Sci. Rep.* 6:21242. doi: 10.1038/srep21242
- Wang, Y., Reddy Satyavolu, N. S., and Lu, Y. (2018). Sequence-specific control of inorganic nanomaterials morphologies by biomolecules. *Biol. Colloids Interfaces* 38, 158–169. doi: 10.1016/j.cocis.2018.10.009
- Xu, Y., Lu, Y., Zhang, P., Wang, Y., Zheng, Y., Fu, L., et al. (2020). Infrageneric phylogenetics investigation of *Chimonanthus* based on electroactive compound profiles. *Bioelectrochemistry* 133:107455. doi: 10.1016/j.bioelechem.2020.107455
- Yang, N., WeiHong, L., and Hao, L. (2014). Biosynthesis of Au nanoparticles using agricultural waste mango peel extract and its in vitro cytotoxic effect on two normal cells. *Mater. Lett.* 134, 67–70. doi: 10.1016/j.matlet.2014.07.025
- Yu, B., Liu, Y., Zhang, J., Hai, T., Li, B., Lu, P., et al. (2016). Electrochemical analysis of nicotine based on multi-walled carbon nanotube/graphene composite. *Int. J. Electrochem. Sci.* 11, 4979–4987. doi: 10.20964/2016.06.68
- Zhang, H., and Hu, X. (2019). Biosynthesis of au nanoparticles by a marine bacterium and enhancing their catalytic activity through metal ions and metal oxides. *Biotechnol. Prog.* 35:e2727. doi: 10.1002/btpr.2727
- Zheng, Y., Wang, Z., Peng, F., and Fu, L. (2017). Biosynthesis of silver nanoparticles by *Plectranthus amboinicus* leaf extract and their catalytic activity towards methylene blue degradation. *Rev. Mex. Ing. Quím.* 16, 41–45.
- Zhu, A., Qiao, L., Tan, P., Zeng, W., Ma, Y., Dong, R., et al. (2019). Boosted electrocatalytic activity of nitrogen-doped porous carbon triggered by oxygen functional groups. *J. Colloid Interface Sci.* 541, 133–142. doi: 10.1016/j.jcis.2019.01.077

**Conflict of Interest:** SN, MC, YD, and LZ were employed by the company Changde Branch of Hunan Tobacco Corporation. JL and QZ were employed by the company Sichuan of China National Tobacco Corporation.

The remaining authors declare that the research was conducted in the absence of any commercial or financial relationships that could be construed as a potential conflict of interest.

Copyright © 2020 Jing, Ning, Guan, Cao, Li, Zhu, Zhang, Cheng and Deng. This is an open-access article distributed under the terms of the Creative Commons Attribution License (CC BY). The use, distribution or reproduction in other forums is permitted, provided the original author(s) and the copyright owner(s) are credited and that the original publication in this journal is cited, in accordance with accepted academic practice. No use, distribution or reproduction is permitted which does not comply with these terms.